Thermoelectric Signatures of Time-Reversal Symmetry Breaking States in Multiband Superconductors

Julien Garaud, Mihail Silaev, and Egor Babaev
Department of Theoretical Physics and Center for Quantum Materials, KTH-Royal Institute of Technology, Stockholm SE-10691, Sweden

(Received 16 July 2015; revised manuscript received 17 November 2015; published 4 March 2016)

We show that superconductors with broken time-reversal symmetry have very specific magnetic and electric responses to inhomogeneous heating. A local heating of such superconductors induces a magnetic field with a profile that is sensitive to the presence of domain walls and crystalline anisotropy of superconducting states. A nonstationary heating process produces an electric field and a charge imbalance in different bands. These effects can be measured and used to distinguish $s+is$ and $s+id$ superconducting states in the candidate materials such as $Ba_{1-x}K_xFe_2As_2$.

DOI: 10.1103/PhysRevLett.116.097002

In many recently discovered superconducting materials, the pairing of electrons is supposed to take place in several sheets of a Fermi surface formed by overlapping electronic bands [1–6]. Of special interest are the states where the difference of gap's phases in the bands is neither 0 or π [7–18]. Indeed, in addition to the breakdown of usual U(1) gauge symmetry, such superconducting states are characterized by an extra broken time-reversal symmetry (BTRS) that has numerous interesting physical consequences, many of which are not yet explored. Iron-based superconductors [3] are among the most commonly accepted candidates for the observation of a BTRS state originating from the multiband character of superconductivity and several competing pairing channels.

Experimental data suggest that in the hole-doped 122 compounds $Ba_{1-x}K_xFe_2As_2$ the symmetry of the superconducting state can change depending on the doping level x. At moderate doping $x\sim 0.4$ various measurements including neutron scattering [19], thermal conductivity [20], and angle-resolved photoemission spectroscopy (ARPES) [21–23] are consistent with the hypothesis of the $s_\pm$ state where the superconducting gap changes sign between electron and hole pockets. On the other hand, the symmetry of the superconducting state at heavy doping $x\to 1$ is not so clear regarding the question of whether the d channel dominates or if the gap retains $s_\pm$ symmetry changing sign between the inner hole bands at the Γ point [24,25]. Indeed, there is evidence that the d-wave pairing channel dominates [26–29], while other ARPES data were interpreted in favor of an s-wave symmetry [30,31].

Which of these two possibilities is realized at heavy doping depends on the fine balance of the pairing interactions in different channels. However, both cases strongly suggest the existence of an intermediate superconducting state that breaks time-reversal symmetry at a certain range of the doping level x. Two alternative scenarios have been considered: namely, $s+id$ and $s+is$ symmetries [8,9,17,30,31]. The $s+id$ state is anisotropic, as it breaks C_4 crystalline symmetry, while the $s+is$ state is qualitatively different as C_4 symmetry is preserved [17]. Note that the $s+id$ state is qualitatively different from the (time-reversal-preserving) $s+d$ state which earlier attracted interest in the context of high-temperature cuprate superconductors (see, e.g., [32–35]). It also contrasts with the $d+id$ state that violates both parity and time-reversal symmetries [7,36].

To this day, no experimental proof of $s+is$ or $s+id$ BTRS states has been reported. Indeed, probing the relative phases between components of the order parameter in different bands is a challenging task. For example, the $s+is$ state does not break point group symmetries and therefore it is not associated with intrinsic Cooper pair angular momentum. Hence, it cannot produce a local magnetic field and is invisible for conventional methods like muon spin relaxation and the polar Kerr effect measurements that were used to search for a BTRS $p+ip$ superconducting state in, e.g., the Sr_2RuO_4 compound [37]. Proposals for indirect observation of a BTRS signature in pnictides, with various limitations, have been recently voiced. These include, for example, the investigation of the spectrum of collective modes which includes massless [14] and mixed phase-density [15,17,38,39] excitations. It was also proposed to consider exotic topological excitations in the form of Skyrmions and domain walls [40–42], an unconventional vortex viscosity mechanism [43], vortex clustering [15], and the exotic reentrant and precursor phases induced by fluctuations [44–47]. Spontaneous currents were predicted to exist near impurities in anisotropic superconducting states [8,18] or in samples subjected to strain [18]. The latter proposal actually involves the symmetry change of $s+is$ states and relies on the presence of disorder, which usually has an uncontrollable distribution.

In this Letter, we discuss an experimental setup based on a local heating, that allows the direct observation of BTRS

states in a controllable way. This is illustrated in Fig. 1, where local heating induces a local variation of relative phases that are further shown to yield electromagnetic excitations. The key idea is based on the recent proposal of an unconventional thermoelectric effect in BTRS multiband superconductors [48]. There, a temperature gradient generates phase gradients of condensate components, due to the generically temperature-dependent interband phase differences $\theta_{ki}(T) \coloneqq \theta_k - \theta_i$ (where k, i are band indices). It results that the local heating generates spontaneous magnetic fields and charge imbalance distributions. These thermoelectric responses are drastically different from their counterparts in conventional superconductors [49]. As discussed below, the fields created by local heating have opposite directions in two degenerate superconducting states [i.e., $s + is(d)$ and $s - is(d)$ ones]. They are measurable by conventional techniques (e.g., by SQUID) and therefore scans of the surface can be used to diagnose the structure of order parameter and interband phase differences, to detect pinned domain walls or broken crystalline symmetry states in either $s + is$ or $s + id$ superconductors.

We consider a minimal three-band microscopic model which has been suggested to describe the BTRS superconducting state in the hole-doped 122 iron-pnictide compounds [10,17,39] with three distinct superconducting gaps $\Delta_{1,2,3}$ in different bands. The pairing which leads to the BTRS state is dominated by the competition of different interband repulsion channels described by the following coupling matrix:

$$\hat{g} = -\nu_0 \begin{pmatrix} 0 & \eta & \lambda \\ \eta & 0 & \lambda \\ \lambda & \lambda & 0 \end{pmatrix}. \tag{1}$$

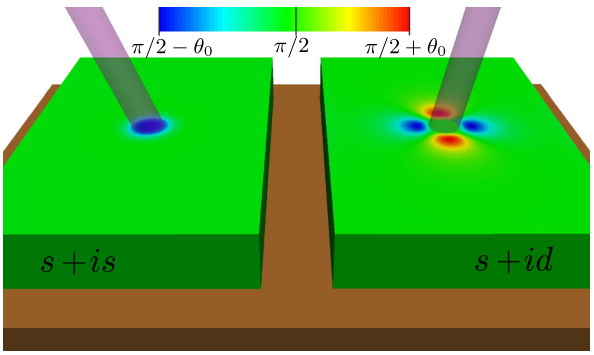

FIG. 1. Variation of the interband phase difference θ_{12} in BTRS three-band superconductors induced by a hot spot created, e.g., by a laser pulse. The phase difference variation induced by temperature gradients around hot spots in the case of an $s + is$ state (left) preserves C_4 symmetry, while it has fourfold structure for an $s + id$ state. The value of θ_0 in the $s + is$ case is 0.18, while for $s + id$ it is smaller: $\theta_0 = 0.05$.

Here, we assume for simplicity that the density of states ν_0 is the same in all superconducting bands. This model has been suggested [10,17,39] in order to describe transitions between $s/s_\pm$ and $s + is$ states when tuning parameters η,λ and temperature. The dimensionless coefficients η and λ describe different pairing channels, whether it is an $s + is$ or an $s + id$ state. In the former case, $\Delta_{1,2}$ correspond to the gaps at hole Fermi surfaces and Δ_3 is the gap at the electron pockets, so that $u_{hh} = \nu_0\eta$ and $u_{eh} = \nu_0\lambda$ are, respectively, the hole-hole and electron-hole interactions [17,39]. The same model (1) can be used to describe the $s + id$ states but there, $\Delta_{1,2}$ describe gaps in electron pockets and Δ_3 is the gap at the hole Fermi surface, so that $u_{eh} = \nu_0\lambda$ and $u_{ee} = \nu_0\eta$ are electron-hole and electron-electron interactions, respectively.

To study magnetic and electric responses of both $s + is$ and $s + id$ states, we use a time-dependent Ginzburg-Landau (TDGL) approach [50,51] generalized to a multiband case [52]. The dimensionless TDGL equations read (see details in [58])

$$(\partial_t + 2i\tilde{e}\varphi)\psi_k = -\frac{\delta\mathcal{F}}{\delta\psi_k^*}, \qquad \boldsymbol{\nabla}\times\boldsymbol{B} - \sigma_n\boldsymbol{E} = \boldsymbol{j}_s, \tag{2}$$

where φ is the electrostatic potential, σ_n is the normal state conductivity, and $\boldsymbol{j}_s = -\delta\mathcal{F}/\delta\boldsymbol{A}$ is the superconducting current. Near the critical temperature the energy relaxation is determined by the phonon scattering which yields the relaxation time scale $t_0 = \pi\hbar/(8T_c) \sim 1$ ps provided $T_c \sim 1$ meV, which is about 10 K.

Note that multiband superconductors are described by several components ψ_k which do not necessarily coincide with the gap functions Δ_i in different bands (see, e.g., [17,39]). For example, since the coupling matrix (1) has only two positive eigenvalues, the relevant Ginzburg-Landau (GL) theory reduces to a two-component one [52], which in dimensionless units reads as

$$\mathcal{F} = \frac{\boldsymbol{B}^2}{8\pi} + \sum_{j=1}^{2}\left(k_j|\Pi\psi_j|^2 + \alpha_j|\psi_j|^2 + \frac{\beta_j}{2}|\psi_j|^4\right) \tag{3a}$$

$$+ k_{12,a}(\Pi_a^*\psi_1^*\Pi_a\psi_2 + \text{c.c.}) \tag{3b}$$

$$+ \gamma|\psi_1|^2|\psi_2|^2 + \frac{\delta}{2}(\psi_1^{*2}\psi_2^2 + \text{c.c.}), \tag{3c}$$

with $\Pi = \boldsymbol{\nabla} - 2i\tilde{e}\boldsymbol{A}$. The components $\psi_{1,2}$ are determined by a superposition of the different gap functions Δ_i. All coefficients of the model (3) are consistently determined from the microscopic coupling matrix (see Supplemental Material [52]), and the temperature dependence is given by the coefficients

$$\alpha_1 = -2(G_0 - G_1 + \tau), \tag{4a}$$

$$\alpha_2 = -(2x^2+1)(G_0 - G_2 + \tau), \tag{4b}$$

where $\tau = (1 - T/T_c)$, $x = (\eta - \sqrt{\eta^2 + 8\lambda^2})/(4\lambda)$, $G_{1,2}$ are the positive eigenvalues of the inverse coupling matrix $\nu_0 \hat{g}^{-1}$ and $G_0 = \min(G_1, G_2)$. The general GL functional (3) derived from the three-band microscopic model has $\delta > 0$. Hence, it favors BTRS with $\pm\pi/2$ phase differences between ψ_1 and ψ_2 order parameter components, which describes both the $s + is$ and $s + id$ states depending on the structure of mixed gradient terms (3b). They are $k_{12,x} = k_{12,y}$ for the $s + is$ state and $k_{12,x} = -k_{12,y}$ for the crystalline C_4-symmetry breaking $s + id$ state.

As a consequence of the discrete degeneracy due to BTRS, the model (3) allows domain walls (DW) interpolating between regions with different relative phases. The direct observation of DWs in $s + is(d)$ states is challenging. Unlike DWs in $p + ip$ superconductors, they do not generate a spontaneous magnetic field. However, by our general argument below, DWs should provide a controlled magnetic response in the presence of relative-density perturbations that can be induced by a local heating.

To investigate the response to spatial modulations of the components of the order parameter induced by a local heat source, the fields $\psi_{1,2}$ and $\boldsymbol{A}$ are discretized using a finite-element framework [55] (see Supplemental Material [52]). To model the local heating, the temperature profile is found by solving the (stationary) heat equation for a heat source at temperature T_s, while boundaries are kept at $T_0 = 0.7T_c$. Once the temperature profile is found, the coefficient α_k in (3) varies in space and the TDGL equations (2) are evolved for $\Delta t = 80$ (in units t_0 defined above). The temperature of the heat source is then modified to T_s', and the TDGL equations are further evolved for the new temperature profile for a period Δt. The temperature of the source is initially set to T_0, sequentially ramped up to $0.95T_c$, and then ramped down back to T_0. In our simulations, we chose the dimensionless conductivity $\sigma_n = 0.1$ and the coupling constant $\tilde{e} = 0.113$. The coefficients in GL functional (3) are determined using the microscopic coupling matrix (1) with coefficients $\eta = 5$ and $\lambda = 4.5$ [59].

As shown in Fig. 2, according to the simulations, when the source heats up a domain wall, it induces a multipolar magnetic field with zero net flux. In the case of a superconductor with $s + is$ symmetry, it shows a dipolar structure, while it is differently distributed for $s + id$. On the other hand, when the heat source is focused on the uniform $s + is$ state it shows no magnetic response, while a fourfold magnetic field is induced in the $s + id$ case as a result of the explicit breakdown of the C_4 symmetry. Here, spatial variations are normalized to the penetration depth λ_L and the amplitudes of the induced magnetic field to the second critical field H_{c2} defined by the GL functional (3). Provided the typical values of $H_{c2} \sim 10$ T in 122 pnictides [60], one can see that the magnetic response can be detected

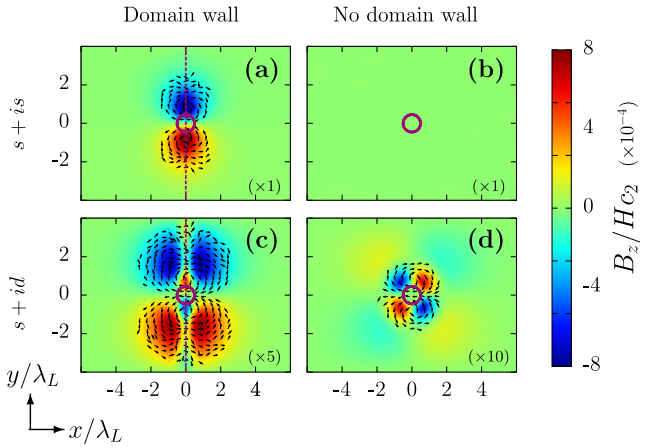

FIG. 2. The magnetic response that originates in local heating of the sample. Panels (a) and (c), respectively, show the response when a local hot spot heats an area of a sample which contains a domain wall. Here, we display two cases of the domain walls for two BTRS states: $s + is$ and $s + id$. Panels (b) and (d) show the response to the local hot spot in the case of the homogeneous BTRS state for the $s + is$ and $s + id$ superconducting state. The color plot shows the magnitude of the out-of-plane induced magnetic field B_z (magnitudes differ in different panels), while arrows indicate the orientation of supercurrents. The dotted line indicates the presence of the domain wall and the inhomogeneous temperature profile is induced by the ringlike heat source shown by the small circles. Length scales are given in terms of London penetration length and calculated values of the GL parameters are given in [52,58,59].

with high accuracy by conventional local probes of static magnetic field such as scanning SQUID or Hall probe microscopy.

The physical origin of the spontaneous magnetic response follows from that the total current is the sum of partial currents in each of the N bands $\boldsymbol{j} = \sum_{k=1}^{N} \boldsymbol{j}_k$ and therefore can generated by the gradients of relative phases [48]. Since $\boldsymbol{j}_k = (\boldsymbol{\nabla}\theta_k - 2\pi\boldsymbol{A}/\Phi_0)c\Phi_0/(8\pi^2\lambda_k^2)$ the London expression for the magnetic field in multiband superconductors is modified as follows:

$$\boldsymbol{B} = -\frac{4\pi}{c}\boldsymbol{\nabla} \times (\lambda_L^2 \boldsymbol{j}) + \frac{\Phi_0}{2\pi N}\sum_{k>i} \boldsymbol{\nabla} \times (\gamma_{ki}\boldsymbol{\nabla}\theta_{ki}), \tag{5}$$

where λ_k are coefficients characterizing the contribution of each band to the Meissner screening, $\lambda_L = 1/\sqrt{\sum_k \lambda_k^{-2}}$ is the London penetration depth, and $\gamma_{ki}(\boldsymbol{r}) = \lambda_L^2[\lambda_k^{-2}(\mathbf{r}) - \lambda_i^{-2}(\mathbf{r})]$. In contrast to London's magnetostatics, Eq. (5) shows that the magnetic field features an additional contribution when relative density gradients $\boldsymbol{\nabla}\gamma_{ki}(\boldsymbol{r})$ are noncollinear with that of relative-phase gradients $\boldsymbol{\nabla}\theta_{ki}$. Such gradients generically appear in BTRS states if a domain-wall-containing superconductor is exposed to a local heat source. The second term in (5) can be nonzero even in the absence of domain walls due to

direction dependent tensor coefficients $\hat{\gamma}_{ki}(\mathbf{r})$ in anisotropic $s+id$ states.

Domain walls can be created by quenching the sample and stabilized by pinning or artificial geometric barriers [42,61]. Yet it is also important to obtain the evidence of isotropic $s+is$ states for homogeneous superconducting states. Below, we show that this can be done by considering the nonequilibrium electric responses generated by nonstationary heating when the local temperature evolves recovering from the initial hot spot created, e.g., by a laser pulse [49]. An unusual electric response can be seen when combining Eq. (5) to Faraday's law. The electric field $\boldsymbol{E}=-c^{-1}\partial_t\boldsymbol{A}-\boldsymbol{\nabla}\varphi$ can be rewritten as

$$\boldsymbol{E}=\frac{4\pi}{c^2}\frac{\partial}{\partial t}(\lambda_L^2\boldsymbol{j})-\frac{\Phi_0}{2\pi Nc}\sum_{k>i}\frac{\partial}{\partial t}(\gamma_{ki}\boldsymbol{\nabla}\theta_{ki})-\boldsymbol{\nabla}\Phi. \qquad (6)$$

Here, $\Phi=\sum_k(\varphi+\hbar\dot{\theta}_k/2e)/N$ is a gauge invariant potential field, determined by the sum of chemical potential differences between quasiparticles $\mu_q=e\varphi$ and condensates in each band $\mu_p^{(k)}=-\hbar\dot{\theta}_k/2$. Each of the partial potential differences $\Phi^{(k)}=[\mu_q-\mu_p^{(k)}]/e$ is proportional to charge imbalance in the kth band $Q_k^*=2e^2\nu_0\Phi^{(k)}$ [62–64]. In multicomponent systems the charge imbalance can be generated by variations of interband phase differences in space and time. The physics behind this process is a nonequilibrium redistribution of Cooper pairs between different bands which initially creates partial charge imbalances Q_k^*. This mechanism leads to the unconventional electric response of BTRS superconductors to a nonstationary local heating. It can be measured with potential probe techniques that were employed to study the imbalance between quasiparticles and condensate subsystems in conventional superconductors [65,66].

Figure 3 shows such an electric response to a nonstationary heating of the superconducting sample. This multicomponent electrodynamic phenomenon can be used to detect BTRS states through charge imbalance generation in response to nonstationary heating. As shown in Fig. 3, the charge imbalance shows a nontrivial pattern that is different for $s+is$ and $s+id$ states. The total charge imbalance $\langle\Phi\rangle$ in uniform $s+id$ is zero as a result of the fourfold symmetric structure due to broken C_4 symmetry. On the other hand, as shown in Fig. 3(e), $\langle\Phi\rangle\neq 0$ in uniform $s+is$. Note that the total imbalance in the case of domain walls Figs. 3(a) and 3(c) is zero because the heat source is centered at the domain wall. A shifted source from the DW center will not be symmetric and thus its average will not vanish.

The generated charge imbalance can be measured with the standard technique using the normal metal and superconducting potential probes [65,66]. The magnitude of voltage V_N induced in the normal detector is related to the dimensionless signal shown in Fig. 3 as $V_N=h\Phi/(t_0e)$,

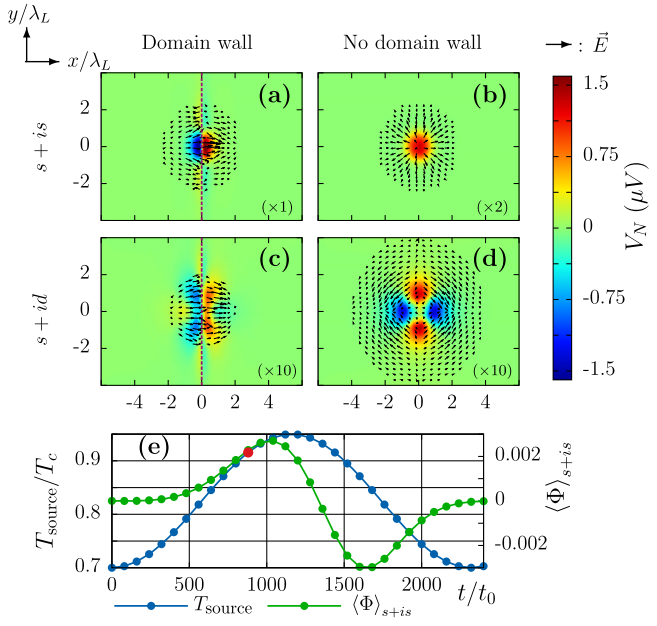

FIG. 3. Electric response due to the nonstationary heating of the sample. Panel (e) shows the time evolution of the source's temperature. Panels (a)–(d) correspond to the cases in Fig. 2 and the color plot shows the voltage V_N generated by the charge imbalance that can be picked by a normal detector, while the arrows correspond to the electric field. Panel (e) also displays Φ integrated over the whole sample, of an $s+is$ superconductor without DW (b). The red dot on panel (e) denotes the "position" of panels (a)–(d) in the time series.

where $h/(t_0e)\approx 4$ mV. The overall magnitude of the voltage signal is thus expected at the order of the μV. The electric field and charge imbalance depend on the dynamics of the temperature profile variation, while $\boldsymbol{B}$ depends on the temperature profile itself. As a result, the sign of the induced electric field and charge imbalance changes when ramping down the heat-source temperature, while it does not for the magnetic field (see animations in the Supplemental Material [52]). Note that similarly to the spontaneous magnetic field, the induced charge imbalances are sensitive to BTRS: degenerate $s+is$ and $s-is$ states produce opposite electric fields and charge imbalances in response to the same heating protocol. It allows us to discriminate between the usual thermoelectric occurring in conventional superconductors and the unconventional one being a specific signature of BTRS states.

To conclude, we demonstrated possible direct manifestations of BTRS states in experimentally observable electric and magnetic responses to nonuniform and nonstationary heating. The signs of the generically induced magnetic field and charge imbalance distributions are opposite in degenerate BTRS states [i.e., in $s+is(d)$ and $s-is(d)$]. These specific thermoelectric behaviors were also shown to reveal the presence of domain walls between $s+is(d)/s-is(d)$ states. Moreover, the demonstrated crucial dependence of thermomagnetic and charge imbalance responses on

crystalline anisotropy provides an experimental tool to distinguish between isotropic $s+is$ and C_4 symmetry-breaking $s+id$ states that are particularly interesting for pnictides.

The work was supported by the Swedish Research Council Grants No. 642-2013-7837. The computations were performed on resources provided by the Swedish National Infrastructure for Computing (SNIC) at the National Supercomputer Center at Linköping, Sweden.

[1] I. I. Mazin and V. P. Antropov, Electronic structure, electron-phonon coupling, and multiband effects in MgB_2, Physica (Amsterdam) **385C**, 49 (2003).

[2] A. Damascelli, D. H. Lu, K. M. Shen, N. P. Armitage, F. Ronning, D. L. Feng, C. Kim, Z.-X. Shen, T. Kimura, Y. Tokura, Z. Q. Mao, and Y. Maeno, Fermi Surface, Surface States, and Surface Reconstruction in Sr_2RuO_4, Phys. Rev. Lett. **85**, 5194 (2000).

[3] Y. Kamihara, T. Watanabe, M. Hirano, and H. Hosono, Iron-based layered superconductor $La[O_{1-x}F_x]FeAs$ ($x=0.05$–0.12) with $T_c=26$ K, J. Am. Chem. Soc. **130**, 3296 (2008).

[4] I. I. Mazin, D. J. Singh, M. D. Johannes, and M. H. Du, Unconventional Superconductivity with a Sign Reversal in the Order Parameter of $LaFeAsO_{1-x}F_x$, Phys. Rev. Lett. **101**, 057003 (2008).

[5] K. Kuroki, S. Onari, R. Arita, H. Usui, Y. Tanaka, H. Kontani, and H. Aoki, Unconventional Pairing Originating from the Disconnected Fermi Surfaces of Superconducting $LaFeAsO_{1-x}F_x$, Phys. Rev. Lett. **101**, 087004 (2008).

[6] A. V. Chubukov, D. V. Efremov, and I. Eremin, Magnetism, superconductivity, and pairing symmetry in iron-based superconductors, Phys. Rev. B **78**, 134512 (2008).

[7] A. V. Balatsky, Field-induced $d_{x^2-y^2}+id_{xy}$ state and marginal stability of high-T_c superconductor, Physica (Amsterdam) **332C**, 337 (2000).

[8] W.-C. Lee, S.-C. Zhang, and C. Wu, Pairing State with a Time-Reversal Symmetry Breaking in FeAs-Based Superconductors, Phys. Rev. Lett. **102**, 217002 (2009).

[9] C. Platt, R. Thomale, C. Honerkamp, S.-C. Zhang, and W. Hanke, Mechanism for a pairing state with time-reversal symmetry breaking in iron-based superconductors, Phys. Rev. B **85**, 180502 (2012).

[10] V. Stanev and Z. Tešanović, Three-band superconductivity and the order parameter that breaks time-reversal symmetry, Phys. Rev. B **81**, 134522 (2010).

[11] R. M. Fernandes and A. J. Millis, Nematicity as a Probe of Superconducting Pairing in Iron-Based Superconductors, Phys. Rev. Lett. **111**, 127001 (2013).

[12] D. F. Agterberg, V. Barzykin, and L. P. Gor'kov, Conventional mechanisms for exotic superconductivity, Phys. Rev. B **60**, 14868 (1999).

[13] T. K. Ng and N. Nagaosa, Broken time-reversal symmetry in Josephson junction involving two-band superconductors, Europhys. Lett. **87**, 17003 (2009).

[14] S.-Z. Lin and X. Hu, Massless Leggett Mode in Three-Band Superconductors with Time-Reversal-Symmetry Breaking, Phys. Rev. Lett. **108**, 177005 (2012).

[15] J. Carlström, J. Garaud, and E. Babaev, Length scales, collective modes, and type-1.5 regimes in three-band superconductors, Phys. Rev. B **84**, 134518 (2011).

[16] A. M. Bobkov and I. V. Bobkova, Time-reversal symmetry breaking state near the surface of an $s_\pm$ superconductor, Phys. Rev. B **84**, 134527 (2011).

[17] S. Maiti and A. V. Chubukov, $s+is$ state with broken time-reversal symmetry in Fe-based superconductors, Phys. Rev. B **87**, 144511 (2013).

[18] S. Maiti, M. Sigrist, and A. Chubukov, Spontaneous currents in a superconductor with $s+is$ symmetry, Phys. Rev. B **91**, 161102 (2015).

[19] A. D. Christianson, E. A. Goremychkin, R. Osborn, S. Rosenkranz, M. D. Lumsden, C. D. Malliakas, I. S. Todorov, H. Claus, D. Y. Chung, M. G. Kanatzidis, R. I. Bewley, and T. Guidi, Unconventional superconductivity in $Ba_{0.6}K_{0.4}Fe_2As_2$ from inelastic neutron scattering, Nature (London) **456**, 930 (2008).

[20] X. G. Luo, M. A. Tanatar, J.-Ph. Reid, H. Shakeripour, N. Doiron-Leyraud, N. Ni, S. L. Bud'ko, P. C. Canfield, H. Luo, Z. Wang, H.-Hu Wen, R. Prozorov, and L. Taillefer, Quasiparticle heat transport in single-crystalline $Ba_{1-x}K_xFe_2As_2$: Evidence for a k-dependent superconducting gap without nodes, Phys. Rev. B **80**, 140503 (2009).

[21] H. Ding, P. Richard, K. Nakayama, K. Sugawara, T. Arakane, Y. Sekiba, A. Takayama, S. Souma, T. Sato, T. Takahashi, Z. Wang, X. Dai, Z. Fang, G. F. Chen, J. L. Luo, and N. L. Wang, Observation of Fermi-surface-dependent nodeless superconducting gaps in $Ba_{0.6}K_{0.4}Fe_2As_2$, Europhys. Lett. **83**, 47001 (2008).

[22] R. Khasanov, D. V. Evtushinsky, A. Amato, H.-H. Klauss, H. Luetkens, Ch. Niedermayer, B. Büchner, G. L. Sun, C. T. Lin, J. T. Park, D. S. Inosov, and V. Hinkov, Two-Gap Superconductivity in $Ba_{1-x}K_xFe_2As_2$: A Complementary Study of the Magnetic Penetration Depth by Muon-Spin Rotation and Angle-Resolved Photoemission, Phys. Rev. Lett. **102**, 187005 (2009).

[23] K. Nakayama, T. Sato, P. Richard, Y.-M. Xu, T. Kawahara, K. Umezawa, T. Qian, M. Neupane, G. F. Chen, H. Ding, and T. Takahashi, Universality of superconducting gaps in overdoped $Ba_{0.3}K_{0.7}Fe_2As_2$ observed by angle-resolved photoemission spectroscopy, Phys. Rev. B **83**, 020501 (2011).

[24] S. Maiti, M. M. Korshunov, T. A. Maier, P. J. Hirschfeld, and A. V. Chubukov, Evolution of the Superconducting State of Fe-Based Compounds with Doping, Phys. Rev. Lett. **107**, 147002 (2011).

[25] S. Maiti, M. M. Korshunov, T. A. Maier, P. J. Hirschfeld, and A. V. Chubukov, Evolution of symmetry and structure of the gap in iron-based superconductors with doping and interactions, Phys. Rev. B **84**, 224505 (2011).

[26] J.-Ph. Reid, A. Juneau-Fecteau, R. T. Gordon, S. René de Cotret, N. Doiron-Leyraud, X. G. Luo, H. Shakeripour, J. Chang, M. A. Tanatar, H. Kim, R. Prozorov, T. Saito, H. Fukazawa, Y. Kohori, K. Kihou, C. H. Lee, A. Iyo, H. Eisaki, B. Shen, H.-H. Wen, and L. Taillefer, From d-wave to s-wave pairing in the iron-pnictide superconductor

(Ba, K)Fe_2As_2, Supercond. Sci. Technol. **25**, 084013 (2012).

[27] J.-Ph. Reid, M. A. Tanatar, A. Juneau-Fecteau, R. T. Gordon, S. R. de Cotret, N. Doiron-Leyraud, T. Saito, H. Fukazawa, Y. Kohori, K. Kihou, C. H. Lee, A. Iyo, H. Eisaki, R. Prozorov, and L. Taillefer, Universal Heat Conduction in the Iron Arsenide Superconductor KFe_2As_2: Evidence of a d-Wave State, Phys. Rev. Lett. **109**, 087001 (2012).

[28] F. F. Tafti, A. Juneau-Fecteau, M-E. Delage, S. Rene de Cotret, J.-Ph. Reid, A. F. Wang, X.-G. Luo, X. H. Chen, N. Doiron-Leyraud, and L. Taillefer, Sudden reversal in the pressure dependence of T_c in the iron-based superconductor KFe_2As_2, Nat. Phys. **9**, 349 (2013).

[29] F. F. Tafti, J. P. Clancy, M. Lapointe-Major, C. Collignon, S. Faucher, J. A. Sears, A. Juneau-Fecteau, N. Doiron-Leyraud, A. F. Wang, X.-G. Luo, X. H. Chen, S. Desgreniers, Y.-J. Kim, and L. Taillefer, Sudden reversal in the pressure dependence of T_c in the iron-based superconductor $CsFe_2As_2$: A possible link between inelastic scattering and pairing symmetry, Phys. Rev. B **89**, 134502 (2014).

[30] D. Watanabe, T. Yamashita, Y. Kawamoto, S. Kurata, Y. Mizukami, T. Ohta, S. Kasahara, M. Yamashita, T. Saito, H. Fukazawa, Y. Kohori, S. Ishida, K. Kihou, C. H. Lee, A. Iyo, H. Eisaki, A. B. Vorontsov, T. Shibauchi, and Y. Matsuda, Doping evolution of the quasiparticle excitations in heavily hole-doped $Ba_{1-x}K_xFe_2As_2$: A possible superconducting gap with sign-reversal between hole pockets, Phys. Rev. B **89**, 115112 (2014).

[31] K. Okazaki, Y. Ota, Y. Kotani, W. Malaeb, Y. Ishida, T. Shimojima, T. Kiss, S. Watanabe, C.-T. Chen, K. Kihou, C. H. Lee, A. Iyo, H. Eisaki, T. Saito, H. Fukazawa, Y. Kohori, K. Hashimoto, T. Shibauchi, Y. Matsuda, H. Ikeda, H. Miyahara, R. Arita, A. Chainani, and S. Shin, Octet-line node structure of superconducting order parameter in KFe_2As_2, Science **337**, 1314 (2012).

[32] R. Joynt, Upward curvature of H_{c2} in high-T_c superconductors: Possible evidence for $s-d$ pairing, Phys. Rev. B **41**, 4271 (1990).

[33] Q. P. Li, B. E. C. Koltenbah, and R. Joynt, Mixed s-wave and d-wave superconductivity in high-T_c systems, Phys. Rev. B **48**, 437 (1993).

[34] A. J. Berlinsky, A. L. Fetter, M. Franz, C. Kallin, and P. I. Soininen, Ginzburg-Landau Theory of Vortices in d-Wave Superconductors, Phys. Rev. Lett. **75**, 2200 (1995).

[35] V. R Misko, V. M Fomin, J. T Devreese, and V. V Moshchalkov, On the Ginzburg-Landau analysis of a mixed $s-d_{x^2-y^2}$-wave superconducting mesoscopic square, Solid State Commun. **114**, 499 (2000).

[36] M. Franz and Z. Tešanovíc, Self-Consistent Electronic Structure of a $d_{x^2-y^2}$ and a $d_{x^2-y^2}+id_{xy}$ Vortex, Phys. Rev. Lett. **80**, 4763 (1998).

[37] A. P. Mackenzie and Y. Maeno, The superconductivity of Sr_2RuO_4 and the physics of spin-triplet pairing, Rev. Mod. Phys. **75**, 657 (2003).

[38] V. Stanev, Model of collective modes in three-band superconductors with repulsive interband interactions, Phys. Rev. B **85**, 174520 (2012).

[39] M. Marciani, L. Fanfarillo, C. Castellani, and L. Benfatto, Leggett modes in iron-based superconductors as a probe of time-reversal symmetry breaking, Phys. Rev. B **88**, 214508 (2013).

[40] J. Garaud, J. Carlström, and E. Babaev, Topological Solitons in Three-Band Superconductors with Broken Time Reversal Symmetry, Phys. Rev. Lett. **107**, 197001 (2011).

[41] J. Garaud, J. Carlström, E. Babaev, and M. Speight, Chiral $\mathbb{C}P^2$ Skyrmions in three-band superconductors, Phys. Rev. B **87**, 014507 (2013).

[42] J. Garaud and E. Babaev, Domain Walls and Their Experimental Signatures in $s+is$ Superconductors, Phys. Rev. Lett. **112**, 017003 (2014).

[43] M. Silaev and E. Babaev, Unusual mechanism of vortex viscosity generated by mixed normal modes in superconductors with broken time reversal symmetry, Phys. Rev. B **88**, 220504 (2013).

[44] T. A. Bojesen, E. Babaev, and A. Sudbø, Time reversal symmetry breakdown in normal and superconducting states in frustrated three-band systems, Phys. Rev. B **88**, 220511 (2013).

[45] T. A. Bojesen, E. Babaev, and A. Sudbø, Phase transitions and anomalous normal state in superconductors with broken time-reversal symmetry, Phys. Rev. B **89**, 104509 (2014).

[46] J. Carlström and E. Babaev, Spontaneous breakdown of time-reversal symmetry induced by thermal fluctuations, Phys. Rev. B **91**, 140504 (2015).

[47] A. Hinojosa, R. M. Fernandes, and A. V. Chubukov, Time-Reversal Symmetry Breaking Superconductivity in the Coexistence Phase with Magnetism in Fe Pnictides, Phys. Rev. Lett. **113**, 167001 (2014).

[48] M. Silaev, J. Garaud, and E. Babaev, Unconventional thermoelectric effect in superconductors that break time-reversal symmetry, Phys. Rev. B **92**, 174510 (2015).

[49] A. Maniv, E. Polturak, G. Koren, Y. Bliokh, B. Biehler, B.-U. Runge, P. Leiderer, B. Shapiro, and I. Shapiro, Observation of a New Mechanism of Spontaneous Generation of Magnetic Flux in a Superconductor, Phys. Rev. Lett. **94**, 247005 (2005).

[50] N. Kopnin, *Theory of Nonequilibrium Superconductivity*, International Series of Monographs on Physics (Oxford University Press, Oxford, 2009), ISBN 9780198507888.

[51] A. T. Dorsey, Vortex motion and the Hall effect in type-II superconductors: A time-dependent Ginzburg-Landau theory approach, Phys. Rev. B **46**, 8376 (1992).

[52] See Supplemental Material at http://link.aps.org/supplemental/10.1103/PhysRevLett.116.097002, which includes Refs. [50,53–57], for detailed derivations and animations of the nonstationary processes.

[53] A. B. Vorontsov, I. Vekhter, and M. Eschrig, Surface Bound States and Spin Currents in Noncentrosymmetric Superconductors, Phys. Rev. Lett. **101**, 127003 (2008).

[54] D. Saint-James, E. J. Thomas, and G. Sarma, *Type II Superconductivity*, International Series of Monographs in Natural Philosophy (Pergamon Press, Oxford, 1970), ISBN 978-0080123929.

[55] F. Hecht, New development in freefem^{++}, J. Numer. Math. **20**, 251 (2012).

[56] N. S. Manton and P. Sutcliffe, *Topological Solitons* (Cambridge University Press, Cambridge, U.K., 2004), p. 493.

[57] R. Rajaraman, *Solitons and Instantons. An Introduction to Solitons and Instantons in Quantum Field Theory* (North-Holland Publishing Company, Amsterdam, 1982).

[58] The lengths are normalized by $\tilde{\xi}_0 = \hbar \bar{v}_F / T_c$, where $\bar{v}_F$ is the average value of Fermi velocity, magnetic field by $B_0 = T_c \sqrt{\nu_0/\rho}$, where T_c is in energy units, and $\rho = 7\zeta(3)/(8\pi^2) \approx 0.1$. The magnetic field scale B_0 is of the order of the thermodynamic critical field at low temperatures [54]. In such units the electron charge is replaced by an effective coupling constant $\tilde{e} = \pi B_0 \xi_0^2 / \Phi_0$.

[59] The consistently obtained values are $\beta_1 = 2$, $\beta_2 = 1.108$, $\delta = 0.465$, and $\gamma = 0.929$. The coefficients of the kinetic terms are $k_1 = 0.55$, $k_2 = 0.375$, and $k_{12,x} = 0.217$, while $k_{12,y} = k_{12,x}$ for $s + is$ states and $k_{12,y} = -k_{12,x}$ for $s + id$. See Supplemental Material [52] for a detailed derivation.

[60] G. R. Stewart, Superconductivity in iron compounds, Rev. Mod. Phys. **83**, 1589 (2011).

[61] P. J. Curran, S. J. Bending, W. M. Desoky, A. S. Gibbs, S. L. Lee, and A. P. Mackenzie, Search for spontaneous edge currents and vortex imaging in Sr_2RuO_4 mesostructures, Phys. Rev. B **89**, 144504 (2014).

[62] T. J. Rieger, D. J. Scalapino, and J. E. Mercereau, Charge Conservation and Chemical Potentials in Time-Dependent Ginzburg-Landau Theory, Phys. Rev. Lett. **27**, 1787 (1971).

[63] M. Tinkham and J. Clarke, Theory of Pair-Quasiparticle Potential Difference in Nonequilibrium Superconductors, Phys. Rev. Lett. **28**, 1366 (1972).

[64] A. M. Kadin, L. N. Smith, and W. J. Skocpol, Charge imbalance waves and nonequilibrium dynamics near a superconducting phase-slip center, J. Low Temp. Phys. **38**, 497 (1980).

[65] J. Clarke, Experimental Observation of Pair-Quasiparticle Potential Difference in Nonequilibrium Superconductors, Phys. Rev. Lett. **28**, 1363 (1972).

[66] M. L. Yu and J. E. Mercereau, Nonequilibrium quasiparticle current at superconducting boundaries, Phys. Rev. B **12**, 4909 (1975).